Acta of Bioengineering and Biomechanics
Vol. 23, No. 4, 2021

Original paper
DOI: 10.37190/ABB-01894-2021-02

Predicting pedestrian lower limb fractures in real world vehicle crashes using a detailed human body leg model

ZHEWU CHEN[1], XING HUANG[2]*, DONGHUA ZOU[3], FUHAO MO[4], JIN NIE[5], GUIBING LI[1]

[1] School of Mechanical Engineering, Hunan University of Science and Technology, Xiangtan, China.
[2] Medical Imaging Center, The First People's Hospital of Chenzhou, Chenzhou, China.
[3] Shanghai Key Laboratory of Forensic Medicine, Academy of Forensic Science, Ministry of Justice, Shanghai, China.
[4] State Key Laboratory of Advanced Design and Manufacturing for Vehicle Body, Hunan University, Changsha, China.
[5] Loudi Vocational and Technical College, Loudi, China.

Purpose: The purpose of this study was to evaluate the capability of a detailed FE human body lower limb mode, called HALL (Human Active Lower Limb) model, in predicting real world pedestrian injuries and to investigate injury mechanism of pedestrian lower limb in vehicle collisions. *Methods:* Two real world vehicle-to-pedestrian crashes with detailed information were selected. Then, a pedestrian model combining the HALL model and the upper body of the 50th% Chinese dummy model and vehicle front models were developed to reconstruct the selected real world crashes, and the predictions of the simulations were analyzed together with observations from the accident data. *Results*: The results show that the predictions of the HALL model for pedestrian lower limb long bone fractures match well with the observation from hospital data of the real world accidents, and the predicted thresholds of bending moment for tibia and femur fracture are close to the average values calculated from cadaver test data. Analysis of injury mechanism of pedestrian lower limb in collisions indicates that the relatively sharper bumper of minivan type vehicles can produce concentrated loading to the lower leg and a high risk of tibia/fibula fracture, while the relatively sharper and lower bonnet leading edge may cause concentrate loading to the thigh and high femur fracture risk. *Conclusions*: The findings imply that the HALL model could be used as an effective tool for predicting pedestrian lower limb injuries in vehicle collisions and improvements to the minivan bumper and sedan bonnet leading edge should be concerned further in vehicle design.

Key words: *pedestrian lower limb fracture, vehicle crash, accident reconstruction, human body leg model*

1. Introduction

Lower limb injuries account for more than 30% of AIS2+ injuries in vehicle-to-pedestrian crashes, where long bong fractures are dominant [1], [15], [20]. Previous studies suggested that improving vehicle front-end design is an effective approach for pedestrian lower limb protection and a good understanding of injury mechanisms of long bone fractures in real world impact scenarios can provide important reference [21], [25]. Thus, biomechanical analysis of pedestrian lower limb injury in real world vehicle crashes is still of great significance for vehicle safety design.

Finite element (FE) human body modes have become an important tool in analysis of injury biomechanics [10], [26] and many studies have focused on biomechanical response of pedestrian lower limb under vehicle impact loading [2], [5], [6], [11], [16], [17], [23]. However, the most of existing FE human body lower limb models used in vehicle safety research defined muscles as a single or several simplified blocks without considering of detailed anatomy structures for trans-articular muscles, and were only validated against

* Corresponding author: Xing Huang, Medical Imaging Center, The First People's Hospital of Chenzhou, Chenzhou, China, e-mail: xnyx_tg@163.com
Received: September 24th, 2021
Accepted for publication: October 27th, 2021

Post-Mortem Human Surrogate (PMHS) tests without evaluation from the aspect of predicting real world injuries. For the former issue, Mo et al. [18] developed a human body lower limb-pelvis FE model with detailed 3D active muscles, which was initially validated against data from PMHS and volunteer tests, and employed to investigate Knee-Thigh-Hip (KTH) injury mechanisms and tolerances in vehicle front collisions [18]. This model was then further improved and configured into the standing position to form a pedestrian lower limb model, named as HALL (Human Active Lower Limb) model, which was validated basically against PMHS test data in a recent publication [19]. The HALL model becomes one of the most detailed human body lower limb FE model in the field, and has been applied as an important tool in vehicle safety studies [5], [11], [22]. However, the predictive capability of the HALL model for pedestrian leg injuries in real world crashes has not been assessed. Furthermore, understanding on the injury mechanism of pedestrian lower limb in real world vehicle collisions is still insufficient given the uncertainty of crash scenarios.

Therefore, the purpose of the current work was to evaluate the capability of the HALL model in predicting real world pedestrian injuries and to investigate injury mechanism of pedestrian lower limb in vehicle collisions via numerical reconstruction of two real world vehicle-to-pedestrian crashes. To achieve it, two real world vehicle-to-pedestrian crashes with detailed information were first selected. Then, a pedestrian model combining the HALL model and the upper body of the 50% Chinese dummy model and vehicle front models were developed. Finally, simulations of vehicle-to-pedestrian impact were conducted to reconstruct the selected real world crashes using the pedestrian and vehicle front models and accident information, and the predictions of the simulations were analyzed in somparison with observations from accident data.

2. Materials and methods

2.1. Case summary

Two real-world vehicle-to-pedestrian crashes were selected for reconstruction in this study based on their detail hospital data (X-ray or CT) of lower limb fractures and on-site information. The general information of these two cases are summarized in Table 1, where Case 1 was from the IVAC (In-depth Investigation of Vehicle Accidents in Changsha) database and Case 2 was from Academy of Forensic Science, Ministry of Justice, China. It should be noted that the vehicle impact speeds were calculated from multi-body modeling reconstruction (Case 1) or video data (Case 2). Tibia and femur shaft fractures were observed from hospital data for Case 1 and Case 2, respectively. In Figure 1, the vehicles involved in Case 1 and Case 2 are shown, where the deformation traces for pedestrian tibia (bull bar bumper) and femur (bonnet leading edge) fractures are marked. Both fractures and their sources of contact are typical for vehicle-to-pedestrian crashes, hence, the selected cases are representative.

Table 1. Summary of the crash cases

Case	Category		Details	Source
Case 1	Vehicle	Model	Dongfeng EQ6362PF 2008 (Minivan)	Manufacturer
		Dimension	3640 × 1560 × 1925 mm	
		Mass	985 kg	
		Impact speed	45 km/h	Calculation
	Pedestrian	Age	40 years	Victim
		Height	172 cm	
		Weight	68 kg	
		Leg injury	Right tibia shaft fracture (X-ray)	Hospital
Case 2	Vehicle	Model	Elysee 2015 (Sedan)	Manufacturer
		Dimension	4427 × 1748 × 1476mm	
		Mass	1150 kg	
		Impact speed	65 km/h	Calculation
	Pedestrian	Age	17 years	Victim
		Height	168 cm	
		Weight	65 kg	
		Leg injury	Right femur shaft fracture (CT)	Hospital

(a) (b)

Fig. 1. Vehicles involved in Case 1 (left) and Case 2 (right), where red cycles indicate the deformation traces for lower pedestrian limb fractures

2.2. Pedestrian model

The Human Active Lower Limb (HALL) model, which includes detail skeleton, ligaments and 3D muscles, was employed for predicting pedestrian leg fractures in the current study (Fig. 2). This model was initially developed by researchers from Hunan University based on CT and MRI images from a Chinese male close to the 50th percentile [18], and then was improved further and validated against cadaver tests [19]. In the HALL model, the isotropic elastic-plastic material model, elastic viscoplastic material model, Ogden material model and quasi linear viscoelastic (QLV) material model were defined for cortical bones, spongy bones, muscles and ligaments, respectively [18]. For model validation, dynamic three-point bending tests were employed for validation of the thigh and lower leg models, four-point bending tests and uniaxial loading experiments along the fiber direction were considered for evaluation of the knee joint model, and lateral shear and lateral bending collision experiments were used for validation of the whole lower limb model [19]. To consider the effect of upper body mass on pedestrian lower limb injury risk in vehicle collisions, the HALL model was connected with the upper body of the 50th% Chinese dummy model to form a full-body pedestrian FE model (Fig. 2) for application of vehicle-to-pedestrian crash simulations in Section 2.3.

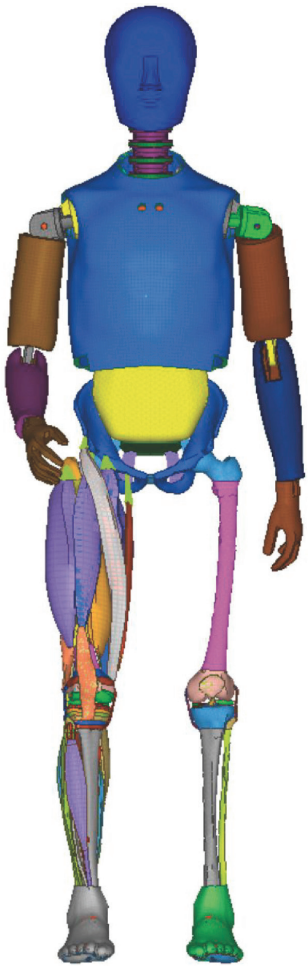

Fig. 2. The pedestrian model combining the Human Active Lower Limb (HALL) model and upper body of the 50th% Chinese dummy model

2.3. Crash reconstruction

Vehicle front FE models (Fig. 3) were used to simulate the selected crashes. For Case 1, a minivan front FE model was extracted from a full-scale FE model of a production minivan, which has the similar design to the accident vehicle and has been used in previous studies of pedestrian safety [9], [24]. The frames and bonnet were modeled by steel materials and plastic material was used for the cover of bumper. Unfortunately, stiffness information about the accident minivan is not available, hence the difference in stiffness between the model and real minivan is not able to be compared due to lack of data, but this difference is not likely to be very big considering the very similar cost of manufacture for vehicles at this level. For Case 2, a sedan front FE model was developed according to the geometry constructed based on the point cloud data obtained from 3D laser scanning of the accident vehicle. The outer shell of the sedan front model was modeled by steel (bonnet) and plastic (bumper) materials similar to the minivan front FE model, and a solid layer with material properties of Expanded Polypropylene Particle (EPP) foam attached to the outer shell was used to control the stiffness of the sedan model according to the performance of this car in Euro-NCAP and the stiffness corridors from impactor tests [12].

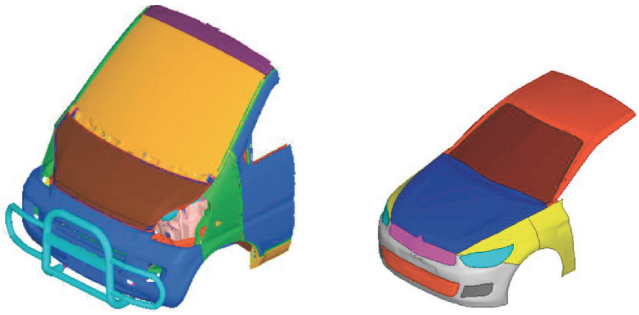

(a) (b)

Fig. 3. Vehicle front FE models of a minivan for Case 1 (a) and a sedan for Case 2 (b)

Vehicle-to-pedestrian impact simulation models were then developed using the above pedestrian and vehicle front FE models (Fig. 4). It is should be noticed that for each case: the pedestrian model was scaled to the height of the victim in the accident according to the information listed in Table 1; the initial contact location and gait stance were defined based on the deformation traces on the accident vehicles (Fig. 1) and injury information; the impact speed was defined according to the case information (Table 1). To control the effect of uncertainties, before the FE reconstruction, we have preformed optimization study using multi-body simulation and GA (genetic algorithm) to find out the vehicle-to-pedestrian impact boundary condition which is close to the real world accident configuration for each case, where the fitness function was defined as to minimize the sum of relative distance for each pedestrian contact location between prediction from the simulation and observation of the real world case. Then the impact boundary condition was defined in the FE reconstruction for each case. Similarly to previous studies [6], [9], a friction coefficient of 0.3 was applied to the contact between pedestrian and vehicle, and 0.7 was defined for ground-to-pedestrian contact. All FE simulations in the cur rent study were performed under the environment of LS-DYNA software.

(a) (b)

Fig. 4. Vehicle-to-pedestrian impact simulation models for Case 1 (a) and Case 2 (b)

3. Results

In Figure 5, the overall kinematics of the HALL model (only the struck leg is shown) in reconstructions of Case 1 and Case 2, respectively, are shown.

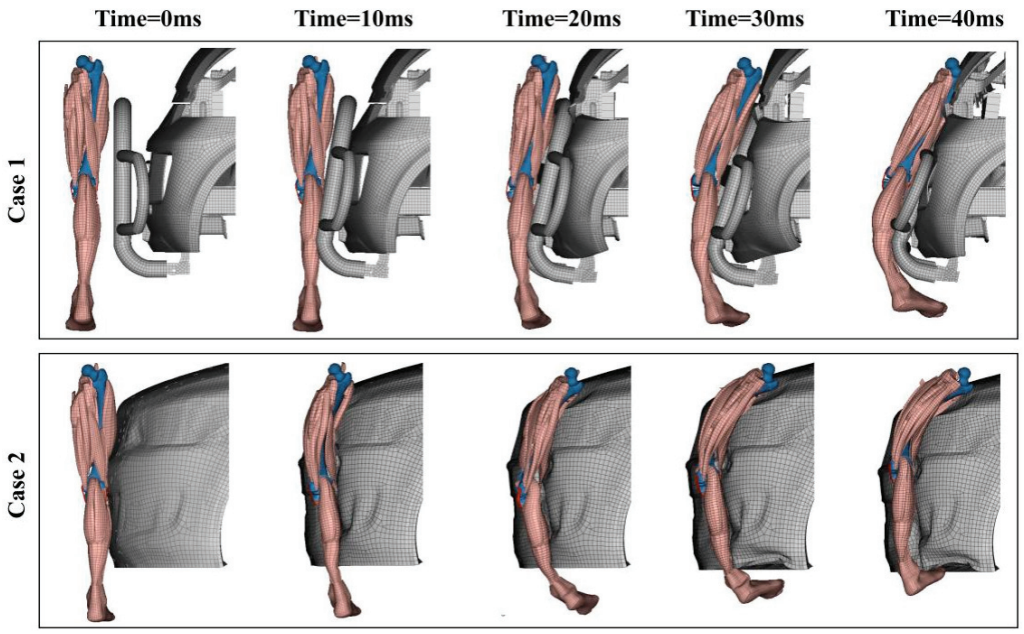

Fig. 5. Predicted kinematics of the HALL model in reconstructions of Case 1 and Case 2 (other body parts are hidden to show clear view of the struck leg)

For Case 1, during the first 20 ms of the impact of the thigh contacts with the upper beam of the bull bar and force it to deform gradually; then, the lower beam of the bull bar struck with the lower leg firmly after the thigh contacts with the bull bar fully, and the lower leg starts to bend until reaching its maximum deformation at 40 ms. For Case 2, the middle rang of the lower limb (shaft thigh-knee-shaft lower leg) contacts with the bumper firstly; then both the thigh and lower leg starts to bend, where the lower leg reaches the maximum bending at 20 ms and the thigh bending continues till 40 ms to reach the maximum deformation. Clearly serious bending occurs to the lower leg and upper leg (thigh) of the HALL model for Case 1 and Case 2, respectively.

As shown in Fig. 6, the deformation traces in the vehicles were compared between the simulations and real world cases. Generally, the locations and characteristics of the predicted deformation traces on the vehicle models can match those of the real world minivan and sedan, though some differences were observed on the bumper deformation for Case 2.

(a) (b)

Fig. 6. Comparison of deformation traces of vehicles between the simulations and real world cases for Case 1 (a) and Case 2 (b)

In Figure 7, the characteristics of long bone fractures between the reconstruction simulations and hospital data from X-ray and CT scan for Case 1 and Case 2, respectively, are compared. The HALL model predicates tibia and fibula fractures in the reconstruction of Case 1, and the location of the predicted frac-

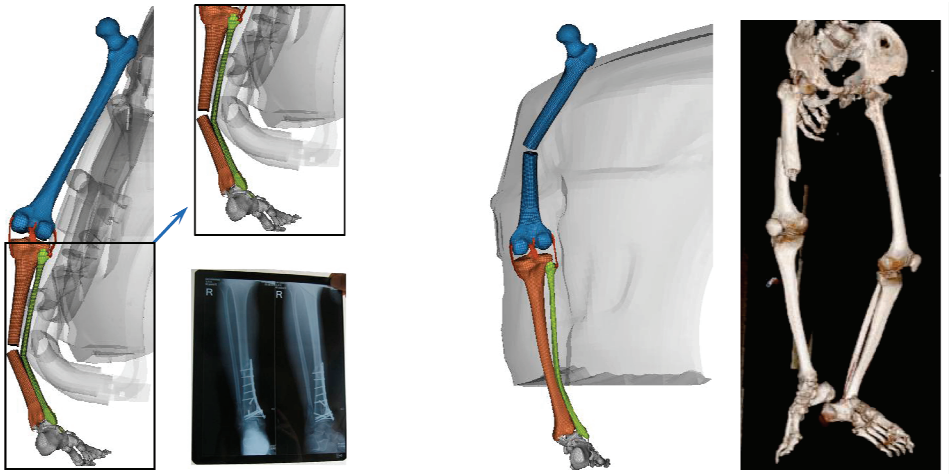

(a) (b)

Fig. 7. Comparison of long bone fractures between the simulation and hospital data for Case 1 (a) and Case 2 (b)

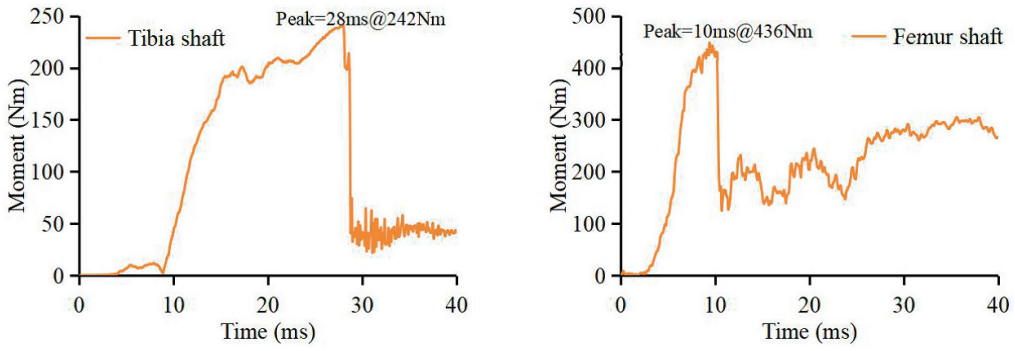

(a) (b)

Fig. 8. Predicted long bone lateral bending moment time history for Case 1 (a) and Case 2 (b)

tures is similar to that of the X-ray data. However, fibula fracture was not observed in the real world case. For Case 2, the HALL model predicates femur shaft fracture, which has the similar location and feature to the CT data.

In Figure 8, the predicted time history of lateral bending moment for the struck leg is shown, where the data for tibia and femur were extracted for Case 1 and Case 2, respectively. The cliff drop of bending moment value in the time history curve indicates the occurrence of long bone fractures in the simulations. The time history data shows that the tibia fracture in the simulation for Case 1 occurred at 28 ms when the tibia bending moment reached the peak value of 242 Nm, while the predicted femur fracture occurred at 10 ms when its bending moment reached the peak value of 436 Nm for Case 2.

In Figure 9, the estimated long bone fracture risk based on the predicted peak bending moment values and the injury risk curves adapted from the study of Kerrigan et al. [3] are shown. In order to reduce the influence of anatomical length on the bending moment value, in the injury risk curves the test data reported by Kerrigan et al. [3] were further scaled using the method similar to previous studies [3], [19], from which the bending moments observed from the tests were scaled to the reference geometry through a scale factor according to the equations below:

$$\lambda_L = L / L_{test}, \tag{1}$$

$$M_{scaled} = \lambda_L^3 M_{test}, \tag{2}$$

where M_{scaled} is the scaled bending moment based on the test data M_{test} and the scale factor λ_L, which is ratio of the length of the model (L) to the anatomical lengths (L_{test}) used to scale all lower leg (378.7 mm) and thigh (448.5 mm) specimens in the tests defined by Kerrigan et al. [3]. According to the length of lower leg and thigh of the scaled HALL model in the reconstructions Case 1 and Case 2, the scale factor for bending moment of tibia and femur fracture risk curves are 0.873 and 0.964, respectively. As can be seen in Fig. 8, the predicted tibia bending moment of 242 Nm for Case 1 reconstruction indicates a risk of tibia fracture floats of 25–65% (average = 45%), while a risk of femur fracture in the rage of 10–100% (average = 53%) are estimated for the simulation of Case 2 according to the predicted peak femur bending moment of 436 Nm.

4. Discussion

4.1. Injury predicting capability of the HALL model

Two real world vehicle-to-pedestrian collisions were reconstructed using the HALL model with detailed anatomy structures, where fractures to the femur and tibia were predicted. Generally the characteristics of the predicted tibia and femur fractures are similar to those observed from the hospital data. However, for the case (Case 1) in which only a tibia fracture was observed in X-ray data the predicted lower limb injuries are not in line with the real world collision, where a fibula fracture (which is non-injured in the real case) was also predicted in the reconstruction (Fig. 7a). This difference may result from the estimated pedestrian posture and/or differences between the minivan front model and the accident vehicle though there are similar in design. But considering the statistical analysis data that the injury type of tibia and fibula combining fracture accounts for 54% in real world vehicle-to--pedestrian collisions and single tibia fracture only

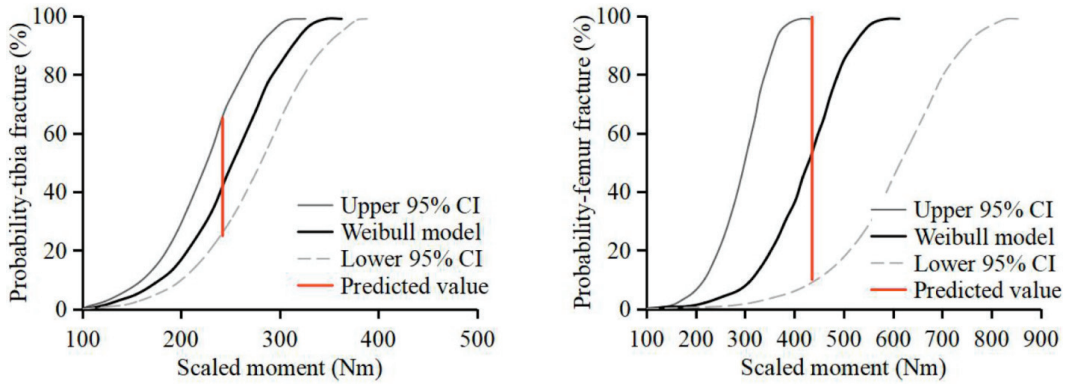

(a) (b)

Fig. 9. Estimated tibia and femur fracture risk for Case 1 (a) and Case 2 (b), respectively

account for 24% [20], the HALL model predicted the most common leg long bone fracture type. The similar prediction of tibia and fibula combining fracture was also observed for the THUMS model in the reconstruction of the same accident case [9]. The results in Figs. 8 and 9 show that the predicted fracture bending moment to tibia is 242 Nm for the HALL model, which refers to a risk of 25–65% tibia fracture according to the scaled injury risk curve adapted from Kerrigan et al. [3]. This predicted tibia fracture threshold of bending moment (242 Nm) is close to the average value of 250 Nm in the risk curve (Fig. 9). For femur fracture prediction, the HALL model simulated similar femur fracture to the real world case (Fig. 7b), and the predicted femur fracture bending moment of 436 Nm is also close to the average value of 430 Nm in the risk curve (Fig. 9). The above findings suggest that the HALL model has acceptable capability in predicting pedestrian's lower limb fractures in real world vehicle collisions.

4.2. Injury mechanism of pedestrian lower limb

In Figure 5, it is shown that pedestrian's lower limb kinematics vary from vehicle front shape, which leads to differences in injury outcome. In particular, tibia and fibula fractures occurred in the minivan impact case due to concentrated loading from the contact with the lower beam of the bull bar, while concentrated loading from the contact with the bonnet leading edge in the sedan impact case resulted in femur fracture to the pedestrian. To illustrate the injury mechanism of pedestrian's lower limb in impacts with different vehicle fronts, in Fig. 10, the approximate loading condition on the pedestrian's lower limb in impacts with typical minivan and modern sedan shape vehicles are shown, where F_{vehicle}, F_{upper} and F_{lower} indicate the reaction forces from vehicle contacts and inertia forces from the upper body mass and the body part below the lower edge of bumper, respectively. The main reaction forces to pedestrian's lower limb are from contacts of lower leg to lower bumper, knee to bumper center and thigh to bonnet leading edge. For minivan shape vehicles, the relatively vertical bonnet and rounded bonnet leading edge can reduce concentrated loading to the thigh, but the relatively sharper and higher bumper (especially when a bull bar is equipped) leads concentrated loading to the lower leg and more serious bending to the knee, which may raise the risk of tibia and fibular fractures. Modern sedan shape cars usually have a flat and wide bumper system, which evenly leads contact to the middle range leg area (shaft thigh-knee-shaft lower leg) and, hence, causes less bending to the knee and lower leg, but the relatively sharper and lower bonnet leading edge can produce concentrate loading to the thigh and a high femur fracture risk. The above understanding of injury mechanism of pedestrian's lower limb matches the injury observation from real world accidents and simulations in the current study, and is also in line with the perspective from previous analyses [2], [5], [6], [13], [14]. The above findings suggest that improvements to the minivan bumper and sedan bonnet leading edge should be concerned further in future vehicle design, and shape optimization and stiffness reduction to these structures might be helpful according to previous studies [4], [5], [7], [13], [14].

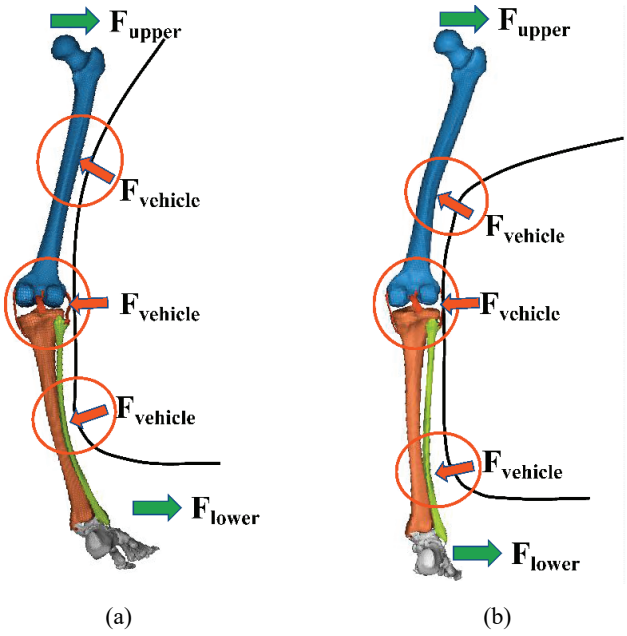

Fig. 10. Loading condition of pedestrian's lower limb in the collision with a minivan type front (a) and sedan type front (b)

4.3. Limitations

There are several limitations to this study. Only two crashes were reconstructed due to lack of detailed hospital data (X-ray and CT) in other cases, reconstructions of more real world cases are needed to further evaluate the injury predicting capability of the HALL model. The pedestrian's posture was approximately estimated based on logical inference and the vehicle front models used here are not exactly the accident vehicles, which could affect pedestrian's dynamic responses and injuries. However, these are inherent drawbacks in reconstruction study of real world collisions. Furthermore, the predicted patterns of the frac-

tures from the HALL model are not the same as those observed from X-ray and CT data (Fig. 7), so the HALL is not able to predict the detailed fracture pattern in real world cases, such as wedge fractures and comminuted fractures, which is also the limitation of FE human body models currently used in vehicle safety analysis. Nevertheless, the predictions of the HALL model are generally plausible given the above uncertainties and inherent drawbacks.

5. Conclusions

Two real world vehicle-to-pedestrian accidents were reconstructed using the HALL model which includes detailed anatomy structures. The results show that the predictions of the HALL model for pedestrian's lower limb long bone fractures match well with the observation from hospital data of the real world accidents reconstructed, and the predicted thresholds of bending moment for tibia and femur fracture are close to the average values calculated from cadaver test data. These findings indicate that the HALL model could be used as an effective tool for predicting pedestrian's lower limb injuries in vehicle collisions. Analysis of injury mechanism of pedestrian lower limb in collisions with different vehicle types indicates that the relatively sharper bumper of minivan type vehicles can produce concentrate loading to the lower leg and a high risk of tibia/fibula fracture, while the relatively sharper and lower bonnet leading edge may cause concentrate loading to the thigh and high femur fracture risk. This finding suggests that improvements to the minivan bumper and sedan bonnet leading edge should be taken into consideration further in vehicle design.

Acknowledgements

This study was supported by Scientific Research Foundation of Hunan Provincial Education Department (Grant Nos. 20B233 and 19C1559) and Natural Science Foundation of Hunan Province, China (Grant Nos. 2020JJ4026 and 2019JJ70045).

References

[1] CHIDESTER C., ISENBERG R., *Final report-the pedestrian crash data study*, Proceedings of the 17th International Technical Conference on the Enhanced Safety of Vehicles (ESV), Amsterdam, Netherlands, 2001.

[2] HAN Y., YANG J., NISHIMOTO K., MIZUNO K., MATSUI Y., NAKANE D., WANAMI S., HITOSUGI M. *Finite element analysis of kinematic behaviour and injuries to pedestrians in vehicle collisions*, Int. J. Crashworthiness, 2012, 17 (2), 141–152.

[3] KERRIGAN J., DRINKWATER D., KAM C., MURPHY D., IVARSSON B., CRANDALL J., PATRIE J., *Tolerance of the human leg and thigh in dynamic latero-medial bending*, Int. J. Crashworthiness, 2004, 9 (6), 607–623.

[4] LI G., WANG F., OTTE D., CAI Z., SIMMS C., *Have pedestrian subsystem tests improved passenger car front shape?*, Accid. Anal. Prev., 2018, 115, 143–150.

[5] LI G., MA H., GUAN T., GAO G., *Predicting safer vehicle front-end shapes for pedestrian lower limb protection via a numerical optimization framework*, Int. J. Auto. Tech.-Kor., 2020, 21 (3), 749–756.

[6] LI G., YANG J., SIMMS C., *The influence of gait stance on pedestrian lower limb injury risk*, Accid. Anal. Prev., 2015, 85, 83–92.

[7] LI G., YANG J., SIMMS C., *Safer passenger car front shapes for pedestrians: a computational approach to reduce overall pedestrian injury risk in real world accident scenarios*, Accid. Anal. Prev., 2017, 100, 97–110.

[8] LI G., LYONS M, WANG B., YANG J., OTTE D., SIMMS C., *The influence of passenger car front shape on pedestrian injury risk observed from german in-depth accident data*, Accid. Anal. Prev., 2017, 101, 11–21.

[9] LI G., TAN Z., LV X., REN L., *Numerical reconstruction of injuries in a real world minivan-to-pedestrian collision*, Acta Bioeng. Biomech., 2019, 21 (2), 21–30.

[10] LINDER A., CLARK A., DOUGLAS C., FILDES B., YANG K., SPARKE L., *Mathematical modeling of pedestrian crashes: review of pedestrian models and parameter study of the influence of the sedan vehicle contour*, 2004 Road Safety Research, Policing and Education Conference, Perth, Australia, 2004.

[11] MA H., MAO Z., LI G., YAN L., MO F., *Could an isolated human body lower limb model predict leg biomechanical response of Chinese pedestrians in vehicle collisions*, Acta Bioeng. Biomech., 2020, 22 (3), 117–129.

[12] MARTINEZ L., GUERRA L., FERICHOLA G., GARCIA A., YANG J., *Stiffness corridors of the European fleet for pedestrian simulation*, Proceedings of the 20th International Technical Conference on the Enhanced Safety of Vehicles (ESV), Lyon, France, 2007.

[13] MATSUI Y., *Effects of vehicle bumper height and impact velocity on type of lower extremity injury in vehicle-pedestrian accidents*, Accid. Anal. Prev., 2005, 37 (4), 633–640.

[14] MATSUI Y., ISHIKAWA H., SASAKI A., *Pedestrian injuries induced by the bonnet leading edge in current car-pedestrian accidents*, SAE Technical Paper No. 1999-01-0713, 1999.

[15] MIZUNO Y., *Summary of IHRA pedestrian safety WG activities (2005)-proposed test methods to evaluate pedestrian protection afforded by passenger cars*, Proceedings of the 19th International Technical Conference on the Enhanced Safety of Vehicles (ESV), Paper No. 05-0138, 2005.

[16] MO F., ARNOUX P., CESARI D., MASSON C., *Investigation of the injury threshold of knee ligaments by the parametric study of car-pedestrian impact conditions*, Saf. Sci., 2014, 62, 58–67.

[17] MO F., ARNOUX P., JURE J., MASSON C., *Injury tolerance of tibia for the car-pedestrian impact*, Accid. Anal. Prev., 2012, 46, 18–25.

[18] MO F., LI F., BEHR M., XIAO Z., ZHANG G., DU X., *A lower limb-pelvis finite element model with 3D active muscles*, Ann. Biomed. Eng., 2018, 46 (1), 86–96.

[19] MO F., LUO S., TAN Z., SHANG B., LV X., ZHOU D., *A human active lower limb model for Chinese pedestrian safety evaluation*, J. Bionic Eng., 2021, 18, 1–15.

[20] OTTE D., HAASPER C., *Characteristics on fractures of tibia and fibula in car impacts to pedestrians and bicyclists-influences of car bumper height and shape*, Annual Proceedings/Association for the Advancement of Automotive Medicine, 2007, 51, 63–79.

[21] SIMMS C., WOOD D., *Pedestrian and Cyclist Impact – A Biomechanical Perspective*, Springer, 2009.

[22] TAN Z., GUO Y., LI G., YAN L., *Kinematics and injury mechanism of cyclist lower limb in vehicle-to-bicycle collisions*, J. Mech. Med. Biol., 2020, 20 (6), 2050035.

[23] UNTAROIU C., YUE N., SHIN J., *A finite element model of the lower limb for simulating automotive impacts*, Ann. Biomed. Eng., 2012, 41, 1–14.

[24] WANG F., WU J., HU L., YU C., WANG B., HUANG X., MILLER K., WITTEK A., *Evaluation of the head protection effectiveness of cyclist helmets using full-scale computational biomechanics modelling of cycling accidents*, J. Safety Res., 2021, DOI: 10.1016/j.jsr.2021.11.005.

[25] YANG J., *Review of injury biomechanics in car–pedestrian collisions*, Int. J. Veh. Saf., 2005, 1 (1/2/3), 100–117.

[26] YANG K., *Basic Finite Element Method as Applied to Injury Biomechanics*, Elsevier, 2018.